Yousri M. A. Welaya
M. Mosleh
Nader R. Ammar

THERMODYNAMIC ANALYSIS OF A COMBINED SOLID OXIDE FUEL CELL WITH A STEAM TURBINE POWER PLANT FOR MARINE APPLICATIONS

Summary

The paper presents a combined system to be operated in ship power plants. The system consists of a solid oxide fuel cell (SOFC) and a steam turbine system which utilizes the energy transported with the exhaust gas leaving the fuel cell. The analyzed variant of the combined cycle includes a SOFC and a steam turbine with a single-pressure waste heat boiler. The calculations are performed for two types of SOFC, tubular and planar, each of power output of 18 MW. The assumptions and limits used in the calculations are also presented. The energy optimization of the entire combined ship power plant is carried out, only from a thermodynamic view point. Technical and economic aspects are not taken into consideration. It is found that a high overall efficiency approaching 60% may be achieved with an optimum configuration using SOFC system. The combined system would also reduce emissions, fuel consumption, and improve the total system efficiency.

Key words: *Marine steam turbine, Natural gas fuel, Solid oxide fuel cell, combined system, Thermodynamic analysis*

1. Introduction

1.1 Emissions from ships

Ships are responsible for 15% of global NO_x emissions, 6% of global sulphur emissions and 2% of CO_2 emissions from fossil fuels. In addition, they are accountable for some 5-10 % of acid rain in coastal regions [1, 2]. Both national authorities and international organizations develop many restrictive regulations to reduce emissions from ships. Now the rate of emissions is an important factor in the selection of power plants to cope with the international requirements.

The International Maritime Organization (IMO) has introduced greenhouse gas (GHG) emission reduction in its agenda since 1995. The IMO has adopted two different emission indexes for a vessel: the Energy Efficiency Design Index (EEDI) and the Energy Efficiency Operational Indicator (EEOI). Both indexes represent the ratio between emissions, in mass of CO_2, and the transported cargo quantity per sailed distance. Regulations were adopted as an amendment to MARPOL Annex VI in October 2010 [2, 3].

In one hand, with regard to the sulphur oxides the permissible emission has been limited by introducing, in Annex VI, the Rule 14 which regulates the permitted sulphur content in the fuel. The permissible sulphur limits in the fuel, in the global terms and in SOx control areas (SECA), together with the dates of their applicability are shown in Table 1. It is permitted to apply, both globally and in the control areas, the scrubbers to clean the exhaust gas of the sulphur oxides. For example, the alternative for the fuel of sulphur content up to 1.5% must be the equipment cleaning down to the level <6g/kWh (SO_2) [3, 4, and 5].

Table 1 The permissible sulphur content in fuel according to MARPOL convention Annex VI [4]

Date of limit application	Sulphur limits in fuel (%)	
	SECA	Global
by June 2010	1.5	4.5
by July 2010	1.0	
2012		3.5
2015	0.1	
2020 or 2025		0.5

On the other hand, IMO has issued regulations limiting NO_x levels from marine diesel engines as shown in Table 2. These regulations include: Tier I for ships constructed from Jan. 2000 to Dec. 2010, Tier II for ships constructed from Jan. 2011 to Dec. 2015, and Tier III for ships constructed from Jan. 2016 onwards when in a NO_x emission control area (ECA) [3, 4].

Table 2 The permissible NOx emission limits according to MARPOL convention Annex VI

Engine speed (rpm)	NO_x emission limit [g/kWh]	
	Tier II	Tier III
n < 130	14.4	3.4
130 ≤ n < 2000	$44 \times n^{-0.23}$	$9 \times n^{-0.2}$
n ≥ 2000	7.7	1.96

1.2 Meeting emission regulations

The options for compliance with IMO new regulations, according to Lloyd's Register [6], include the use of low sulphur fuels/distillates, HFO with a scrubber, LNG, or other alternative fuels. Lloyd's Register considers all options as feasible, but choice is dependent on commercial considerations including trading pattern and percentage of time in ECA's, cost difference and pay-back time, availability of exhaust steam cleaning technologies, and availability of LNG infrastructure. According to a ship owners' survey made by Lloyd's Register about options for mitigating emissions, most owners consider LNG as the fuel most likely to provide the long term solution.

Germanischer Lloyd (GL) sees large market for fuel cells to replace marine auxiliary power. The installed auxiliary power onboard seagoing vessels has a potential market of approximately 160 GW worldwide and can, in principle, be substituted by fuel cells in order to reduce air emissions[7].

1.3 Natural gas and fuel cell opportunities in the marine field

Natural gas (made up of 70-90% methane) is often highlighted as the cleanest fossil fuel alternative of the diesel oil used for marine internal combustion engines. The cleanliness of LNG fuel is easy to appreciate when one notes it yields 100% reductions in SO_x and Particulate Matter (PM) and 92% reduction in NO_x as compared to diesel fuel. LNG also results in a 25% reduction in CO_2, a major contributor to greenhouse gas (GHG) emissions [8].

Fuel cells (FCs) are electrochemical devices which convert the chemical fuels directly into electrical power. The Solid Oxide Fuel Cells (SOFCs) are among the high temperature fuel cells. They consist of a solid oxide electrolyte made from a ceramic such as yttria-stabilized zirconia (YSZ) which acts as a conductor of oxide ions at temperatures from 600 to 1000°C. This ceramic material allows oxygen atoms to be reduced on its porous cathode surface by electrons, thus being converted into oxide ions, which are then transported through the ceramic body to a fuel-rich porous anode zone where the oxide ions can react with hydrogen or hydrogen rich steams giving up electrons to an external circuit. Therefore, SOFC can be operated either by hydrogen or hydrocarbon reformed fuels [9, 10, and 11]. The North Western University patents of direct hydrocarbon oxidation, which deal with special catalysts and anodes, give the SOFC system the potential to use natural gas directly. This improves the opportunity to bypass the hydrogen fuel source problem [11, 12].

In this paper a parametric study on a solid oxide fuel cell has been conducted and the effect of different parameters on the performance of the SOFC and combined SOFC and steam turbine are discussed.

1.4 NG and SOFC in classification societies and regulations

It is a characteristic of marine fuels and equipment to be approved by one of the members of the International Association of Classification Societies (IACS). Classification societies accepted NG as the only gas that can be used onboard. Det Norske Veritas "DNV", China classification society, and Lloyd's Register "LR" have regulations for natural gas driven ships to increase the safety onboard. The International Gas Code (IGC) [13, 14] provides the general arrangement; gas piping systems, fire detection alarm, gas control, monitoring systems and working pressure in the engine room.

In addition, the American Bureau of Shipping (ABS) has recently released a guide for Propulsion and Auxiliary Systems for Gas Fueled Ships (GFS). Its objectives are to provide criteria for arrangements, construction, installation and operation of machinery, equipment and systems for vessels operating with natural gas as a fuel in order to minimize risks to the vessel, crew and environment [8].

The first rules for using fuel cells were introduced by the Germanischer Lloyd (GL) in 2003, together with the International gas code (IGC) development. In addition, Det Norske Veritas (DNV), Bureau Veritas (BV) and other classification societies are working hard to develop rules for using fuel cells in the marine field [15].

2. 500 kW SOFC model

As mentioned above, solid oxide fuel cell (SOFC) is considered as one of the most promising options for marine applications to achieve IMO emission requirements. SOFC can use natural gas directly as a fuel. For the near future, fuel cell can replace the diesel generator. The 18 MW SOFCPP model parameters are based on a 500 kW SOFC model and 55% fuel utilization coefficient. It consists of 36 internally reformed planar and tubular models of 500 kW connected in series and extrapolated for 18 MW SOFC. The 500 kW SOFCPP model main parameters are listed in Table 3 [10].

Table 3 500 kW SOFC model parameters

Parameter	Value
Plant net power	500 kW
TSOFC inlet temperature	800 ^{o}C
TSOFC outlet temperature	1000 ^{o}C
PSOFC inlet temperature	850 ^{o}C
PSOFC outlet temperature	950 ^{o}C
SOFC fuel utilization coefficient	55%
Component pressure loss	1–3%
Component heat loss	1–2%
Ambient pressure	1 atm
Ambient temperature	25 ^{o}C

3. SOFC operational voltage

Solid oxide fuel cell voltage (V_{cell}) is the difference between cell voltage at no load, which can be called open circuit voltage, and the specific fuel cell irreversibility or voltage drop. The following equation (1) shows the operating voltage of a fuel cell at a current density (i_{den}) [16, 17].

$$V_{cell} = E_o - (i_{den} \times r) - A \times \ln(i_{den}) + m \times e^{(n \times i_{den})} \tag{1}$$

In this equation, E_o is the open circuit voltage, ' i_{den}' is internal current density, 'A' is slope of Tafel curve, 'm' and 'n' are constants, 'r' is specific resistance. Typical values of these constants for a SOFC are given in Table 4.

Table 4 Typical values of over voltage parameters [16].

Constant	Typical Value	Unit
E_o	1.01	V
r	$2.0*10^{-3}$	$k\Omega cm^2$
A	0.002	V
m	$1.0*10^{-4}$	V
n	$8*10^{-3}$	$cm^2 mA^{-1}$

4. SOFC-ST combined system description

In SOFC-ST combined cycle, the air flow to the SOFC is compressed by a compressor operated by a steam turbine, as shown in Fig. 1. The steam turbine in the center of the diagram drives two compressors (one for the air, the other for the fuel gas) and an alternator. The air compressor is needed to drive the air through the preheater, the fuel cell, the afterburner, the boiler, and then out to the final heating system. The gas compressor needs to drive the fuel through the same components and so would be at a somewhat higher pressure. They would not normally compress the gases much above air pressure, and the fuel cell would operate at slightly above the ambient pressure. The natural gas is internally reformed in the fuel cell, but not all the hydrogen is consumed. The remainder is burnt in the afterburner, which raises the temperature of both gas streams. This hot gas is used in a heat exchanger type boiler to raise the temperature of the steam, which drives a turbine that drives the alternator [18, 19].
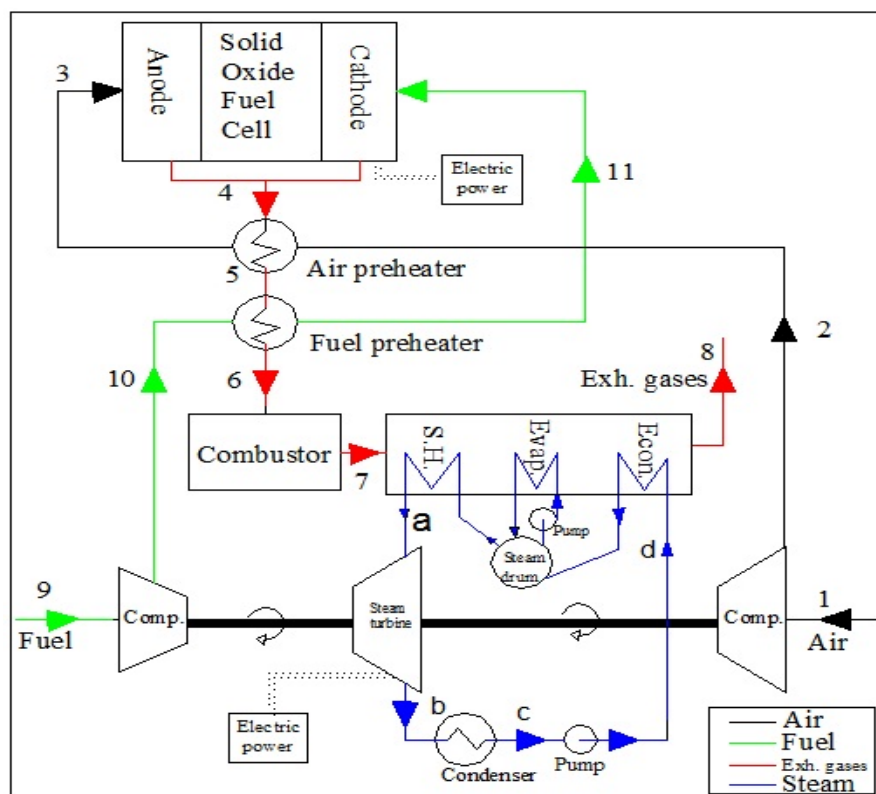
Fig. 1 SOFC-ST combined cycle schematic diagram

5. Energy formulation of components

In the operation of the SOFC, hydrogen fuel is oxidized at the anode, and oxygen is reduced at the cathode to produce electricity, heat and water. The input energy flux to the SOFC should be equal to the output electric energy flux in addition to the other losses as shown in Fig. 2. The total input energy flux, calculated from fuel consumption, in grams per second, using the lower heating value of reacted fuel. The SOFC output electric energy flux is calculated using actual fuel cell current flux and fuel cell stack voltage. The electrochemical efficiency in the SOFC stack is calculated as the ratio between the fuel cell output electric energy flux and the fuel cell input energy flux. Heat energy flux of SOFC can be represented by the energy difference between the actual cell voltage and the ideal cell voltage. This heat energy flux is used to heat the inlet air and fuel streams and to burn unreacted fuels in the combustor. Finally, combustor heat energy flux is incorporated in steam cycle to produce additional electric energy flux which increases the efficiency of SOFC.
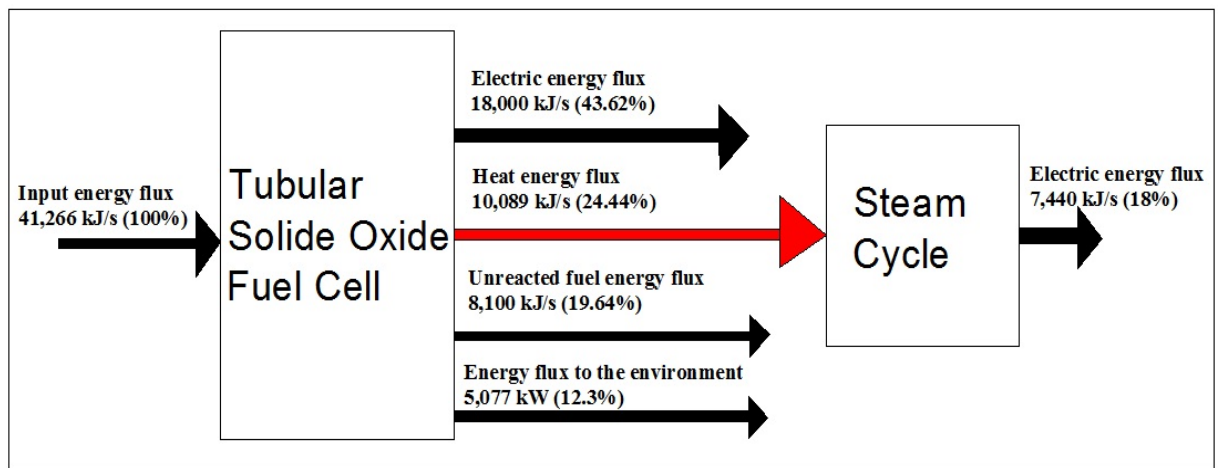
Fig. 2 Schematic of SOFC-ST energy flux

The thermodynamic performance of each of the components introduced in the preceding section will be analyzed here. The mass and energy balance are employed under the assumption of steady flow for the entire cycle. The main stream of the working fluid, assumed as ideal steam, at different states of the cycle is shown in Fig. 1.

A. Air and fuel Compressors

The isentropic efficiency of air and fuel compressors can be defined as:

$$\eta_{aircomp.} = \frac{h_{2S} - h_1}{h_2 - h_1} \tag{2}$$

$$\eta_{fuelcomp.} = \frac{h_{10S} - h_9}{h_{10} - h_9} \tag{3}$$

Where the ideal temperature of the working fluid at the outlet of the compressor can be determined using the following equality:

$$\frac{T_{2S}}{T_1} = \left(\frac{P_2}{P_1}\right)^{(\gamma_{air} - 1)/\gamma_{air}} \tag{4}$$

$$\frac{T_{10S}}{T_9} = \left(\frac{P_{10}}{P_9}\right)^{(\gamma_{gas} - 1)/\gamma_{gas}} \tag{5}$$

Applying the energy balance for the system, the power required for air and fuel compressors may be obtained as follows:

$$P_{aircomp.} = \dot{m}_1 \times (h_2 - h_1) \qquad (6)$$

$$P_{fuelcomp.} = \dot{m}_9 \times (h_{10} - h_9) \qquad (7)$$

B. Fuel and air preheaters

Using the following energy balance equations for air and fuel preheaters, the outlet temperature of the cycle can be determined:

$$\dot{m}_2 \times C_{p_{air}} \times (T_3 - T_2) - \dot{m}_4 \times C_{p_{gas}} \times (T_4 - T_5) \qquad (8)$$

$$\dot{m}_{fuel} \times C_{p_{fuel}} \times (T_{11} - T_{10}) - \dot{m}_5 \times C_{p_{gas}} \times (T_5 - T_6) \qquad (9)$$

C. Solid oxide fuel cell

The fuel supplied to the system is methane (CH_4), with a lower heating value of 50 MJ/kg. The following electrochemical reactions expressed in Eqs. (10 to 12) occur within the anode and cathode of the fuel cell. Various reactions corresponding to the methane are listed below:

$$\text{Reforming: } CH_4 + H_2O \rightarrow CO + 3H_2 \qquad (10)$$

$$\text{Shift gas reaction: } CO + H_2O \rightarrow CO_2 + H_2 \qquad (11)$$

$$\text{Electrochemical: } H_2 + 0.5O_2 \rightarrow H_2O \qquad (12)$$
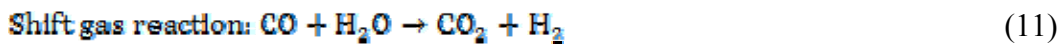
The degree to which an anode supports direct oxidation will then impact the degree of pre-reforming of the fuel that is required, which in turn typically impacts the balance of plant complexity and cost [18, 20]. The net cell reaction is thus written as:

$$CH_{4,anode} + 2O_{2,cathode} \Leftrightarrow 2H_2O_{,anode} + CO_{2,anode} \qquad (13)$$
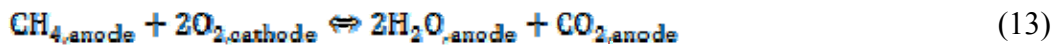
The maximum electrical work obtainable in a fuel cell operating at constant temperature and pressure is given by the change in Gibbs free energy (Δg_f) of the electrochemical reaction. If all the energy from the fuel was transformed into electrical energy, then the reversible open circuit voltage, E_o, would be given by [16, 21]:

$$E_o = \frac{\Delta g_f}{z \times F} \qquad (14)$$

So, the efficiency of fuel cell can be expressed as

$$\eta_{FC} = U_f \frac{V_{cell}}{E_o} \qquad (15)$$

The mass balance for SOFC system gives:

$$\dot{m}_3 + \dot{m}_{fuel} - \dot{m}_4 + \dot{m}_{fuel} \times (1 - U_f) \qquad (16)$$

The last term on the right hand side of the above equality represents the non-reacted mass flow rate that leaves the fuel cell downstream of the products. Using SOFC mass balance, energy fluxes of the inlet and outlet flows of SOFC can be presented as shown in Fig. 3.
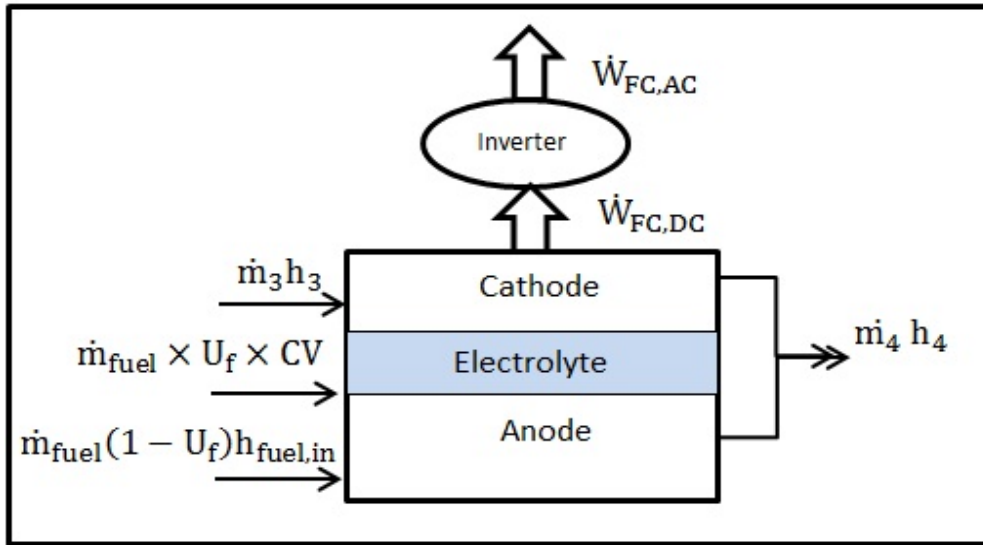
Fig. 3 Schematic of the energy flux of the solid oxide fuel cell with inlet and outlet flows

Applying the first law of thermodynamics to the SOFC and assuming an adiabatic energy process:

$$(\dot{m}_3 \times h_3) + (\dot{m}_{fuel} \times U_f \times CV) + (\dot{m}_{fuel} \times (1 - U_f) \times h_{fuel,in}) = \dot{W}_{FC,DC} + (\dot{m}_4 \times h_4) \qquad (17)$$

D. Combustor

The working fluid of the cycle, with products from the fuel cell, is further heated within the combustor as shown in Fig. 4.
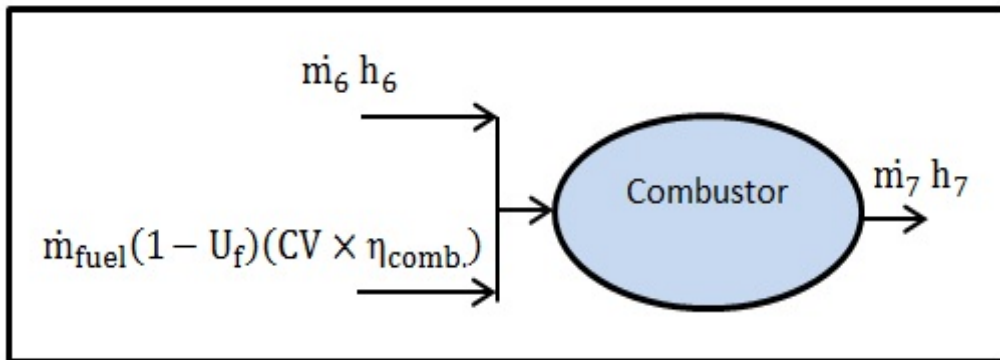
Fig. 4 Schematic of energy flux of the combustor with inlet and outlet flows

Considering that non-reacted flow of fuel from the SOFC is burnt in the combustor and applying the mass balance for combustor gives:

$$\dot{m}_6 + \dot{m}_{fuel} \times (1 - U_f) = \dot{m}_7 \qquad (18)$$

Applying the first law of thermodynamics for the combustor we get:

$$(\dot{m}_6 \times h_6) + (\dot{m}_{fuel} \times (1 - U_f) \times CV \times \eta_{comb.}) = \dot{m}_7 \times h_7 \qquad (19)$$

Where, $\eta_{comb.}$ represents the efficiency of the combustor.

E. Exhaust gas boiler

Typical temperature profiles of exhaust gas and steam/water in the exhaust gas boiler are shown in Fig. 5. The exhaust gas enters the super heater at $\mathbf{T_{go}}$ where the saturated steam is superheated to high temperature $\mathbf{T_{SH}}$. The exhaust gas then enters the evaporator at $\mathbf{T_{g1}}$ where a mixture of saturated water and saturated steam exists. The exhaust gas leaves the evaporator at $\mathbf{T_{g2}}$ and the pinch point (**TPP**) means the temperature difference between $\mathbf{T_{g2}}$ and the saturated temperature $\mathbf{T_{sat}}$. The exhaust gas is discharged to the environment at $\mathbf{T_{g3}}$.
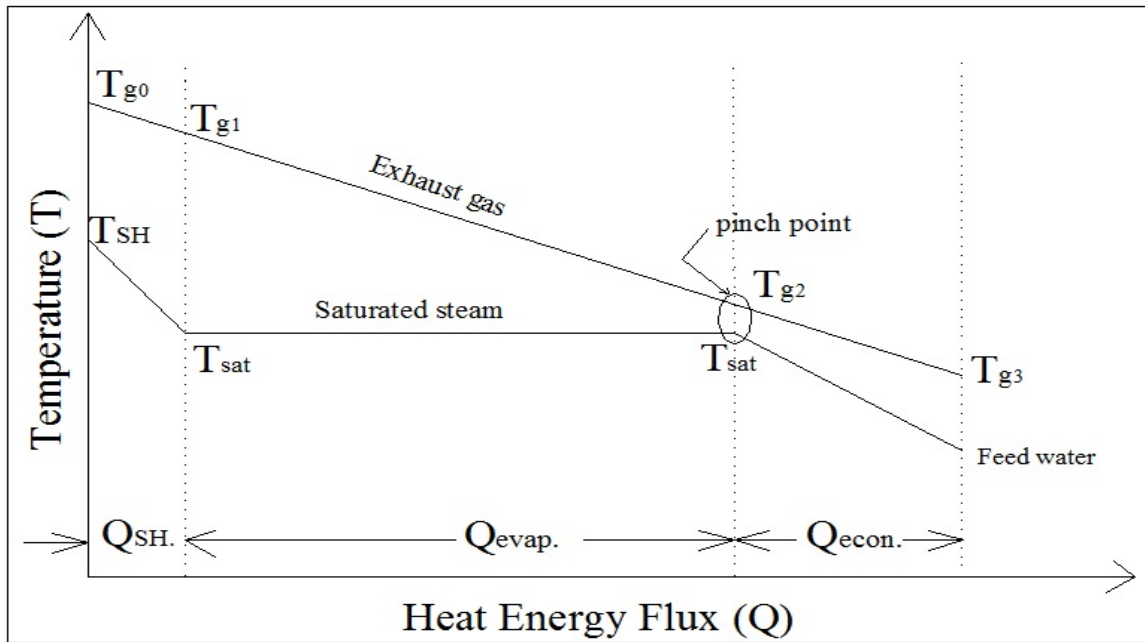
Fig. 5 T-Q diagram for exhaust gas boiler (EGB)

The governing equations for the heat flux available in the gas down to the pinch point (T_{go} to T_{g2}), and the corresponding heat flux absorbed by the superheated and saturated steam are presented below.

$$Q_{SH+Evap.}^{gas} = \dot{m}_{gas} \times C_{p_{gas}} \times (T_{go} - T_{g2}) \tag{20}$$

$$Q_{SH+Evap.}^{steam} = \dot{m}_{steam} \times (h_{superheated} - h_f) \tag{21}$$

Substituting this heat flux value into the steam side equation to solve directly for the steam mass flow rate as in the following equation:

$$Q_{SH+Evap.}^{gas} = Q_{SH+Evap.}^{steam} \tag{22}$$

Knowing the water/steam mass flow rate, the EGB heat flux duty can be calculated using the following equation:

$$Q_{Total}^{steam} = \dot{m}_{steam} \times (h_{superheated} - h_{feedwater}) \tag{23}$$

The gas temperature leaving the EGB (T_{g3}) is now easily calculated, because the total heat flux transferred to the steam is equivalent to that lost by the gas stream:

$$Q_{Total}^{gas} = \dot{m}_{gas} \times C_{p_{gas}} \times (T_{go} - T_{g3}) \tag{24}$$

F. Steam turbine

Knowing EGB heat flux duty, the superheated steam enthalpy (h_a) can be calculated using the following equation:

$$Q_{Total}^{EGB} = \dot{m}_{steam} \times (h_a - h_d) \tag{25}$$

The outlet steam enthalpy of the steam turbine, h_b, can be determined from the definition of isentropic efficiency of the turbine,

$$\eta_{st,isen.} = \frac{h_a - h_b}{h_a - h_{bs}} \tag{26}$$

The required power for natural gas and air compressor is provided by steam turbine power as shown in Fig. 1. So, the steam turbine net power can be calculated using the following equation:

$$P_{stnet} = P_{st} - P_{fuelcomp.} - P_{aircomp.} \tag{27}$$

Where,

$$P_{st} = \dot{m}_{st} \times [(h_a - h_b) - (h_d - h_c)] \tag{28}$$

G. Overall balance equations for integrated cycle

The integrated steam turbine power plant with SOFC in Fig. 1 may be analyzed as a lumped control volume. In the following, mass balance as well as the first and second laws of thermodynamics can be derived from the above mentioned control volume as shown schematically in Fig. 6.

The mass balance for the total system can be written as:

$$\dot{m}_1 + \dot{m}_{fuel} = \dot{m}_8 \tag{29}$$

$$\dot{m}_1 - \dot{m}_2 - \dot{m}_3 \tag{30}$$

$$\dot{m}_7 = \dot{m}_8 \tag{31}$$

Overall energy balance can be expressed as:

$$(\dot{m}_1 \times h_1) + (\dot{m}_{fuel} \times U_f \times CV) + (\dot{m}_{fuel} \times (1 - U_f) \times CV \times \eta_{comb.}) = (\dot{m}_8 \times h_8) + \dot{W}_{FC,DC} + P_{stnet} \tag{32}$$
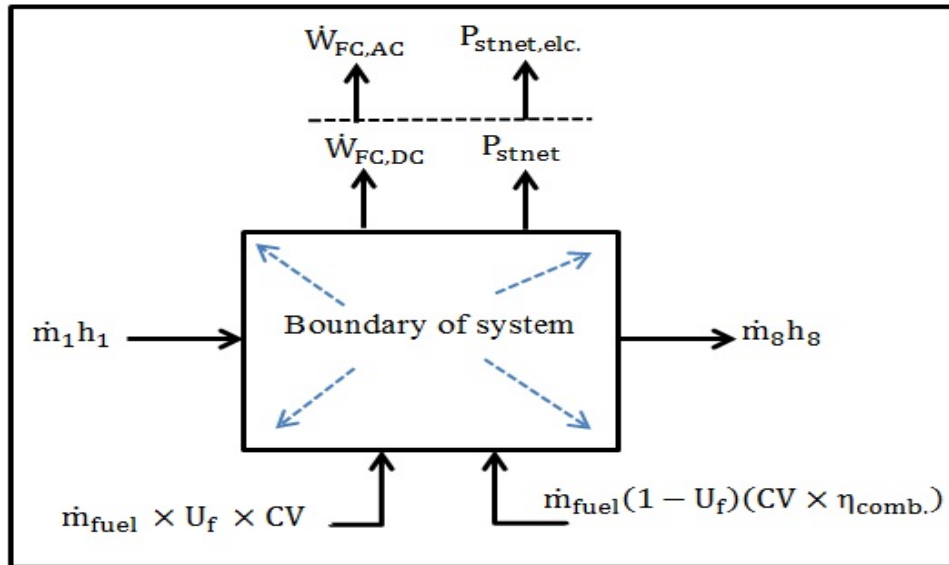
Fig. 6 SOFC–GT cycle as a control volume for the overall energy flux balance

The combined cycle efficiency can be expressed as:

$$\eta_{combined} = \frac{P_{FC,AC} + P_{stnet,elec.}}{\dot{m}_{fuel} \times CV} \tag{33}$$

Where,

$$P_{stnet,elec.} = P_{stnet} \times \eta_{gen.} \tag{34}$$

The steam turbine cycle efficiency can be expressed as:

$$\eta_{st} = \frac{P_{stnet,elec.}}{\dot{m}_{fuel} \times CV} \tag{35}$$

6. Limits of parameters and values assumed in the combined cycle calculations

SOFC-ST combined cycle energy equations are solved using Engineering Equations Solver (EES) program, where the thermodynamic properties of the substances under study can be easily obtained using the built-in functions and data. Analyzing the proposed variant of the combined cycle requires precisely defining particular cycle components. Then, the calculations will be performed taking into account the assumed limits of the parameters and the values selected for the entire combined system utilizing the exhaust gas energy and consisting of the solid oxide fuel cell and the steam turbine system.

The temperature difference (Δt) between the exhaust gas temperature at SOFC exit and the superheated steam temperature in the waste heat boiler in a combined system is assumed equal to $\Delta t = 50\ ^o C$. The "pinch point" value recommended by MAN for boilers is equal to $\Delta t = 10\ ^o C$ [22]. The calculations are performed assuming that the feed water temperature is within $t_{feedwater} = (10–50)\ ^o C$. It is also assumed that the exhaust gas temperature at boiler exit

should be higher than that of the feed water temperature. Moreover, the use of materials revealing extended resistance to acid corrosion is recommended. The lower heating value of the natural gas fuel is assumed equal to 50 MJ/kg.

In addition, this study assumes 55% utilization coefficient of fuel in the cells. Table 5 summarizes the data of different auxiliary system components utilized in the combined SOFC-ST plant.

Table 5 Auxiliary system component data for SOFC-ST plant

Component	Parameter	Value
Air compressor	Isentropic efficiency ($\eta_{aircomp.}$)	85%
Fuel compressor	Isentropic efficiency ($\eta_{fuelcomp.}$)	81%%
Steam turbine	Isentropic efficiency ($\eta_{st,isen.}$)	88%
Combustor	Combustion efficiency ($\eta_{comb.}$)	98%
AC generator	Electric efficiency (η_{gen})	90%
DC/AC Converter	Conversion efficiency	95%
SOFC stack	Pressure loss	3%
Combustor	Pressure loss	2%

7. Comparing the analyzed combined power plant cycles

The performance of a solid oxide fuel cell stack is usually described by the polarization curve, which relates the cell voltage to its current density. This polarization curve is affected by the losses of the fuel cell.

Fig. 7 shows the polarization curve of the SOFC case study. As the cell current increases from zero, there will be a drop of the output voltage of the SOFC. This drop of the cell voltage is due to activation voltage loss. Then, almost a linear decrease of the cell voltage is seen as the cell current increases beyond certain values, as shown in Fig. 7, which is a result of the ohmic loss. Finally, the cell voltage drops sharply to zero as the load current approaches the maximum current density that can be generated by the fuel cell. The sharp voltage drop is the effect of the concentration loss in the fuel cell.
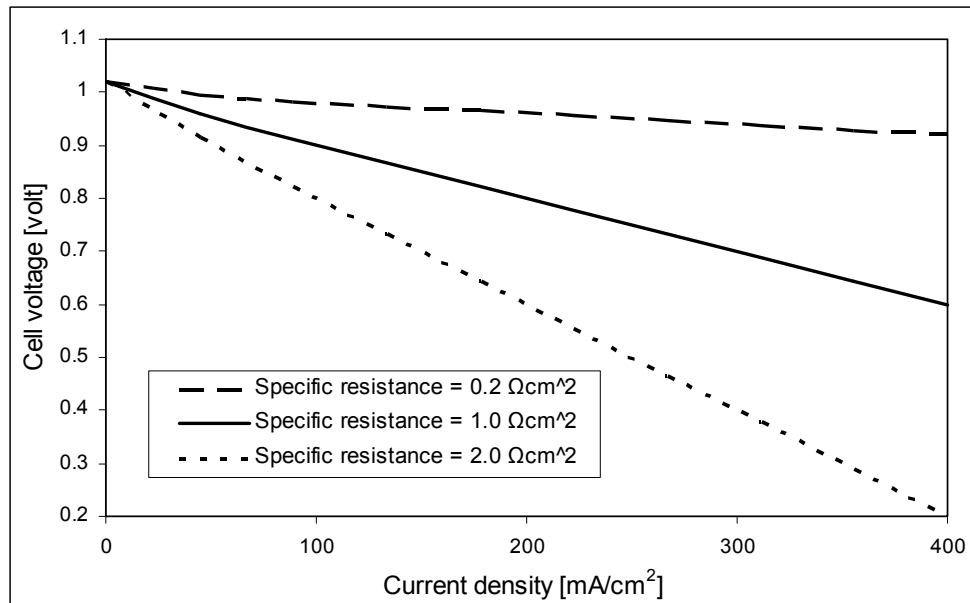
Fig. 7 SOFC voltage at different specific resistance.

The required mass flow rates of hydrogen, oxygen, and air in kg/s are expressed in Eqs. (36, 37 and 38) respectively, and the value of utilization coefficient U_f in Eq. (39) refers to the ratio of hydrogen reacted in the fuel cell [23, 24].

The required hydrogen mass flow rate can be expressed as:

$$m_{hyd.} = \frac{1.05 \times P_{FC,AC}}{10^5 \times V_{cell}}$$
(36)

The required oxygen mass flow rate can be written as:

$$m_{O_2} = \frac{8.29 \times P_{FC,AC}}{10^5 \times V_{cell}}$$
(37)

The required air mass flow rate can be written as:

$$m_{air} = \frac{3.57 \times \lambda_{air} \times P_{FC,AC}}{10^4 \times V_{cell}}$$
(38)

In addition, the hydrogen mass flow rate reacted in fuel cell can be written as:

$$m_{hyd.cons.} = m_{hyd.} \times U_f$$
(39)

The hydrogen formula in Eq. (36) applies only to a hydrogen-fed fuel cell. In the case of a hydrogen/carbon monoxide mixture derived from a reformed hydrocarbon, it will be different. Eq. (40) shows the relationship between the efficiency of the fuel cell, the calorific value "CV in kJ/kg" of the fuel and the resulting fuel rate in kg/s [25].

$$\text{Fuel flow rate} = \frac{P_{FC,AC}}{\eta_{FC} \times CV}$$
(40)

One of the great benefits of the SOFC is that it can utilize a wide range of fuels. The fastest reaction at the nickel anode is that of hydrogen. But other fuels can also react directly on the anode, depending on catalyst composition. In this study two types of SOFCS are included, tubular SOFC (TSOFC), and planar SOFC (PSOFC) using natural gas internal reforming at the cell anode.

The selected operating point for the combined SOFC-ST cycle is at cell output current density of 100 mA/cm^2, cell voltage of 0.801 volts, and fuel utilization coefficient of 55%. At this operating point the mass flow of fuel consumption is 0.236 kg/s and 0.826 kg/s for hydrogen and natural gas respectively. The inlet fuel temperature to SOFC is assumed to be 100°C.

In addition, the mass flow rate of the air used for SOFC-ST cycle depends on the type of fuel used. Air consumption for hydrogen fuel is 32.15 kg/s calculated using Eq. (38), which is nearly half the assumed value if natural gas fuel is used.

Also, the values of the inlet and outlet temperatures of SOFC depend on the type of SOFC modules. For TSOFC the temperatures are 1073 K and 1273 K for the inlet and outlet flows respectively. PSOFC has a higher inlet temperature of 1123 K and a lower outlet temperature of 1223 K compared with TSOFC modules. These values will affect T_3 and T_4 as shown in Fig. 1.

In practical application, the steam turbine system requires some limits imposed on certain parameters resulting from design, constructional and operating assumptions [22, 26]. Using the assumptions adopted in the previous section, the operation of a combined power plant is analysed for solid oxide fuel cell. For combined system an optimal solution was searched in which the power output of the steam turbine reached its maximum. The calculations are performed for three different feed water temperatures, namely 10°C, 30°C and 50°C.

The curves shown in Figs. 8 and 9 illustrate the effect of particular parameters on the steam cycle efficiency. Large differences can be observed in the maximum steam cycle efficiency depending on the selected steam cycle parameters for the SOFC module, whether it is tubular or planar. Moreover, a tendency is observed that the lower the feed water temperature, the higher the steam turbine power.
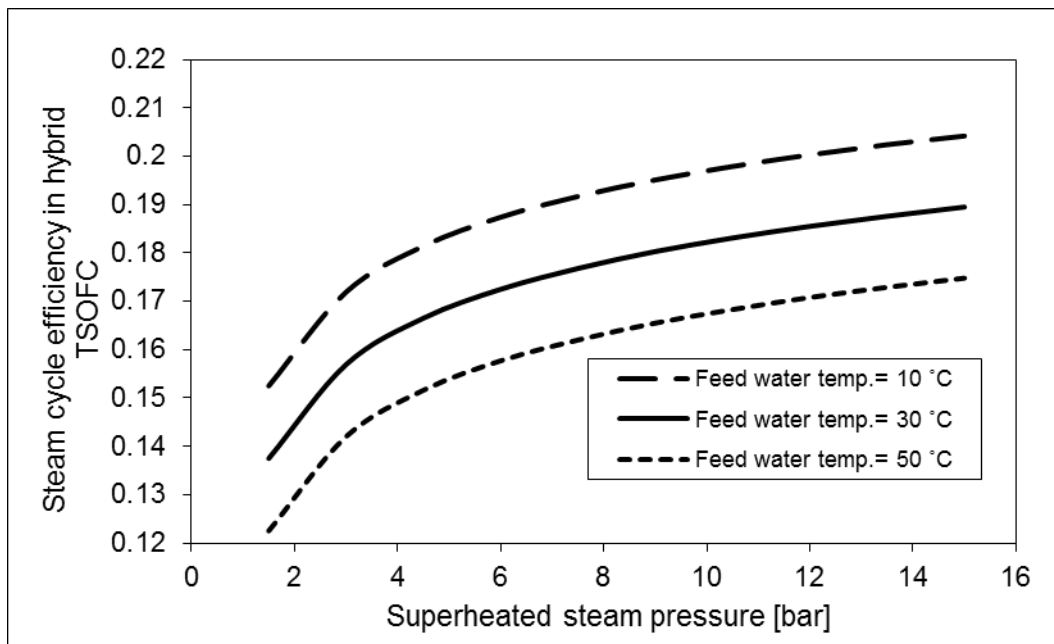
Fig. 8 Steam turbine power output as a function of the superheated steam pressure and the feed water temperature for the TSOFC.
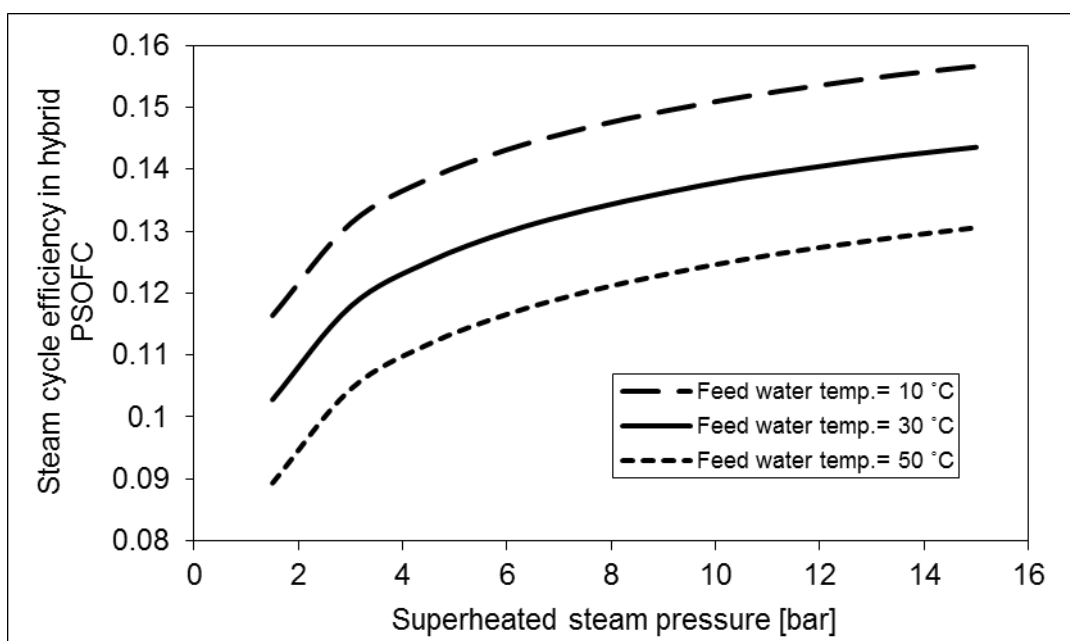
Fig. 9 Steam turbine power output as a function of the superheated steam pressure and the feed water temperature for the PSOFC.

The curves shown in the next Figs. 10 and 11 illustrate the effect of particular parameters on the efficiency of the combined system. Similar to the case of cycle efficiency, it can be observed that the difference in the obtained maximum efficiency of the system depends on the selected solid oxide fuel cell operating parameters. Also, the restrictions concerning the temperature of the feed water and the efficiency of the solid oxide fuel cell working as the main engine in the ship power plant have been taken into consideration.
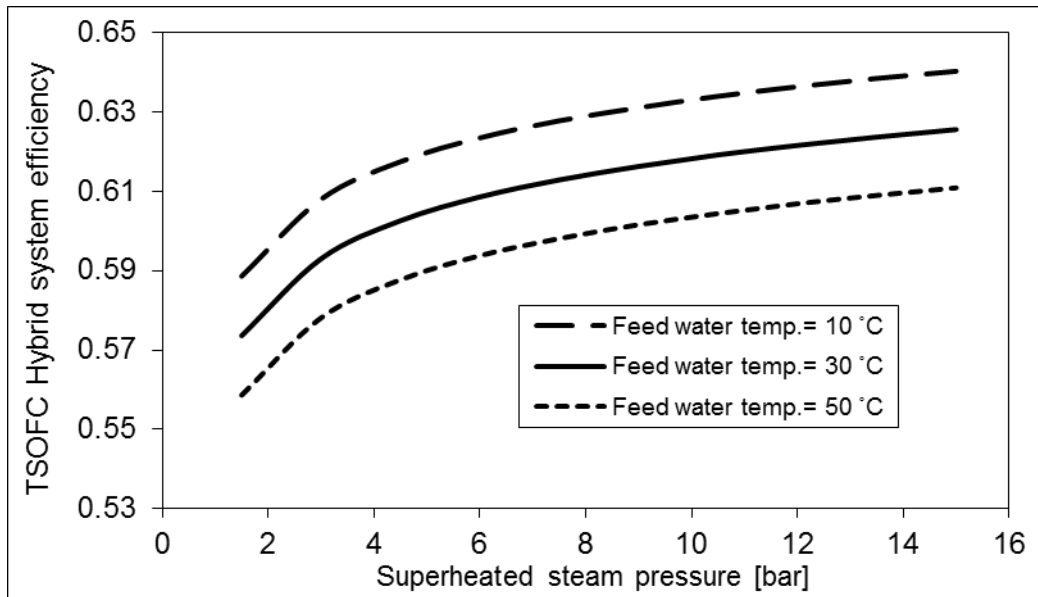
Fig. 10 Efficiency of the combined system as a function of the superheated steam pressure and the feed water temperature for TSOFC
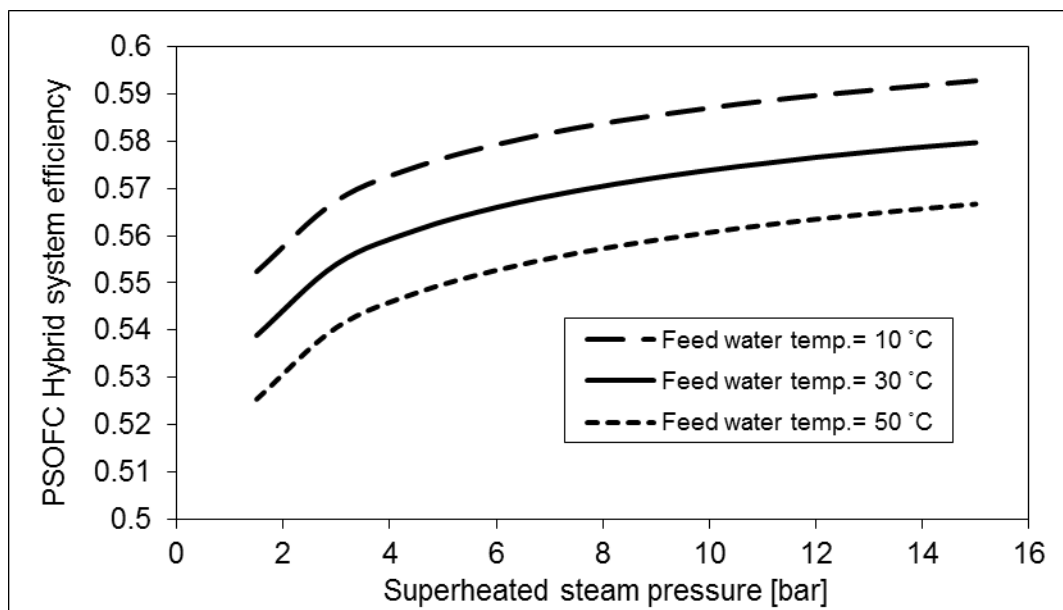
Fig. 11 Efficiency of the combined system as a function of the superheated steam pressure and the feed water temperature for PSOFC

The curves shown in the last two Figs. 12 and 13 illustrate the effect of particular parameters on the exhaust gas temperature behind the waste heat boiler.
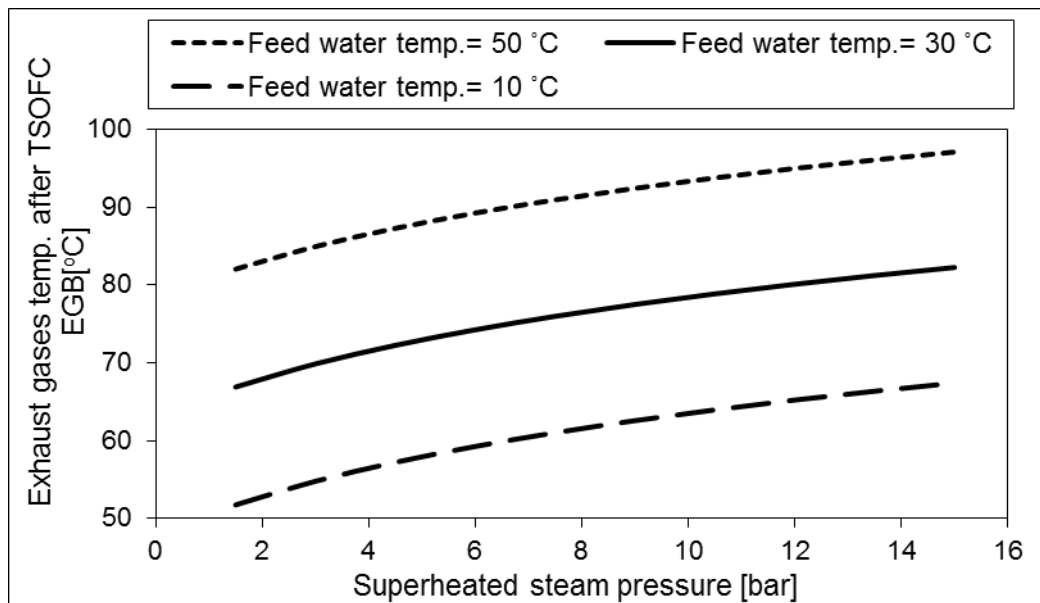
Fig. 12 Exhaust gas temperature at waste heat boiler exit as a function of the superheated steam pressure and the feed water temperature for TSOFC.
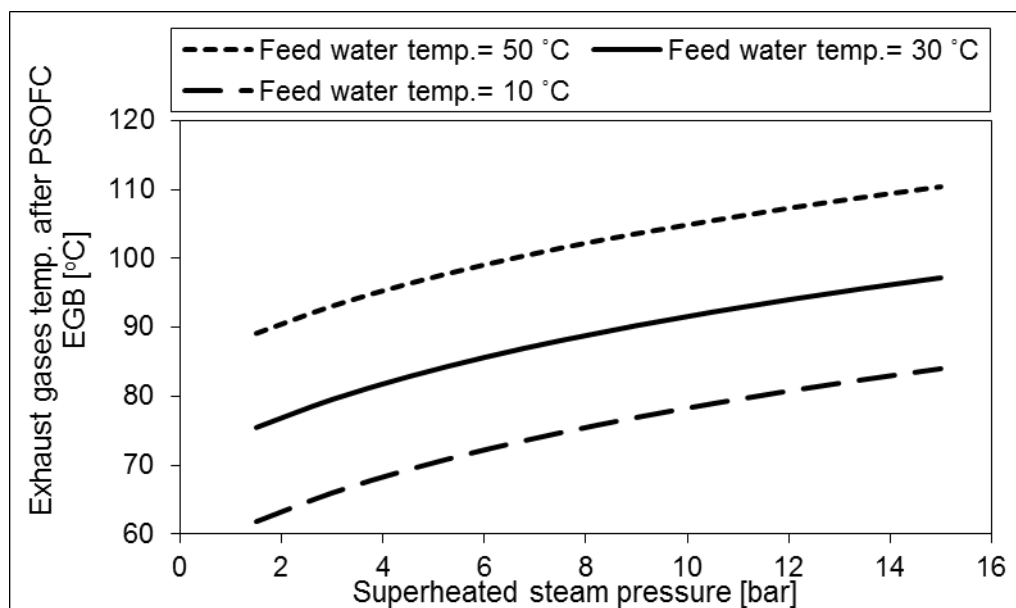
Fig. 13 Exhaust gas temperature at waste heat boiler exit as a function of the superheated steam pressure and the feed water temperature for PSOFC.

Table 6 collects optimal results for the analyzed combined cycle of the ship power plant with tubular and planar SOFC.

Table 6 Results of the combined SOFC and steam turbine cycle taking into account the adapted restrictions

Results of the combined cycle taking into account the adapted restrictions			
Parameter	unit	TSOFC-IR	PSOFC-IR
SOFC power	kW	18000	18000
SOFC efficiency	%	43.62	43.62
SOFC current density	mA/cm^2	100	100
Fuel utilization coefficient	%	55	55
Air compression ratio	%	1.5	1.5

NG compression ratio	%	1.9	1.9
SOFC inlet temp.	°C	800	850
SOFC outlet temp.	°C	1000	950
Feed water temp.	°C	30	30
EGB exhaust temp.	°C	77.5	90.27
Superheated steam pressure	bar	9	9
Condenser pressure	bar	0.04	0.04
steam mass flow rate	kg/s	8.1	7.2
Evaporator pressure	bar	10.5	10.5
Steam turbine net power	kW	7440	5624
Steam cycle efficiency	%	18	13.62
Steam to SOFC power ratio	%	41.33	31.24
Combined efficiency	%	61.62	57.24

The presented results illustrate the power output of the steam turbine which can be reached in the adopted simplest variant of the combined system with a single-pressure waste heat boiler.

Higher efficiency can be reached in the combined cycle with the TSOFC, as compared with the PSOFC. Moreover, the steam mass flow is higher in the combined cycle with the TSOFC than that with the PSOFC.

8. Conclusions

The performed calculations of the combined fuel cell and steam turbine cycle for ship power plants have made it possible to formulate the following conclusions:

- The power output of the combined cycle can be increased, with respect to the conventional power plant, by 41.33% when TSOFC is used as the main engine, and by 31.24% for the PSOFC. No additional fuel consumption is needed for this increase.
- The use of the combined cycle can increase the efficiency of the power plant operating at optimal parameters to 61.62 % in case of the TSOFC and to 57.24% for the PSOFC.
- SOFC engine of lower power output can be used in ship power plant systems in which the additional power is obtained in the combined cycle.

- The paper presents only the thermodynamic analysis of the combined power plant system. It should be complemented by additional technical and economic analysis to fully justify the use of such combined systems in marine power plants.

REFERENCES

[1] James, J.C., et al. Mortality from Ship Emissions: *A Global Assessment. Environmental Science and Technology.* 2007; 4: 24.

[2] Figari, M., D'Amico, M., and Gaggero, P. Evaluation of ship efficiency indexes. *14th Conference of the International Maritime Association of the Mediterranean (IMAM),* Genoa, 2011, pp.621-627.

[3] Greensmith, G. The Legislative Landscape, Lloyd's Register. Middle East and Africa Advisory Technical Committee: www.cdlive.lr.org. 2010.

Thermodynamic analysis of a combined solid oxide fuel cell   Yousri M. A. Welaya, M. Mosleh,

with a steam turbine power plant for marine applications   Nader R. Ammar.

[4]   MEPC. Amendments to the Annex of the Protocol of 1997 to amend the International Convention for the Prevention of Pollution from Ships, 1973- 176(58), as modified by the Protocol of 1978 relating thereto (Revised MARPOL Annex VI), 2011.

[5]   Zenczak, W. The concept of ship's power plant arrangement involving biomass fired boiler, Journal of POLISH CIMAC, 2010; Vol. 5 No. 1, Science publication of Editorial Advisory Board of POLISH CIMAC. ISSN 1231 – 3998, ISBN 83 – 900666 – 2 – 9.

[6]   Farr, J. LNG as a Fuel for Marine Applications. Lloyd's Register. Middle East and Africa Advisory Technical Committee, 2011.

[7]   Barrett, S. GL sees large market for fuel cells to replace marine auxiliary power. Fuel Cells Bulletin, German National Innovation Program for Hydrogen and Fuel Cell Technology: www.now-gmbh.de/index, 2010.

[8]   MAN B&W. Exhaust Gas Emission Control Today and Tomorrow, Application on MAN B&W Two-stroke Marine Diesel Engines. MAN Diesel, Copenhagen, Denmark, 2010.

[9]   Welaya Y MA, El Gohary MM, and Ammar NR. A comparison between fuel cells and other alternatives for marine electric power generation. *International Journal of Naval Architecture and Ocean Engineering (JNAOE)* 2011; 3: 141-149.

[10] Santin M, Traverso A, Magistri L, and Massardo A. Thermo economic analysis of SOFC-GT hybrid systems fed by liquid fuels. *Journal of Energy* 2010; 35: 1077–1083.

[11] Barclay JF. *Fuel Cells, Engines and Hydrogen an Exergy Approach*. John Wiley & Sons Ltd, The Atrium, Southern Gate, Chichester, West Sussex PO19 8SQ, England: 13 978-0-470-01904-7, 2006.

[12] Lisbona, P.U., and Serra, J.L. High-temperature fuel cells for fresh water production. *Journal of Desalination* 2005; 182: 471–482.

[13] IMO-IGC Code, International gas code for construction and equipment of ships carrying liquefied gases in bulk. 2002.

[14] China classification society. Rules for construction and equipment of ships carrying liquefied gases in bulk. Beijing, 2006.

[15] Rattenbury, N., Fort, E. Development of Requirements for Fuel Cells in the Marine Environment Performance and Prescription. Lloyd's Register Technical Papers, 2006.

[16] Larminie, J., Dicks, A. *Fuel Cell Systems Explained*. 2nd Edition, England: John Wiley & Sons Ltd. 0-470-84857-X, 2003, pp.60-91.

[17] Maroju, P. *Modeling of a Fuel Cell*. Master of Science Thesis, Texas Tech University, 2002, p.36.

[18] EG&G Technical Services, Inc. *Fuel Cell Handbook*. Seventh Edition, National Technical Information Service, U. S. Department of Commerce, 2004.

[19] Ghirardo, F., et al. Heat recovery options for onboard fuel cell systems. Journal of Hydrogen Energy, 2011; 36, pp. 8134-8142.

[20] Subhash, C.S., and Kevin, K. (ed.). *High Temperature Solid Oxide Fuel Cells: Fundamentals, Design and Applications*. Elsevier Advanced Technology, The Boulevard, Langford Lane, Kidlington Oxford OX5 lGB, UK, 1856173879, 2004.

[21] Raja, A. K., Srivastava, A. P., and Dwivedi, M. Power Plant Engineering. New Age International (P) Ltd, 2006; pp.20-35.

[22] Olszewski, W. Possible use of combined Diesel engine and steam turbine systems in ship power plants, *Scientific Journals* 2011; 28: 88–94.

[23] Holland, B.J., and Zhu, J.G. Design of A 500 W PEM Fuel Cell Test System. Faculty of Engineering, University of Technology, Sydney, PO Box 123, Broadway, NSW, 2007.

[24] Kumm, W.H. Marine and Naval Applications of Fuel Cells for Propulsion: The Process Selection. *Journal of Power Sources* 1990; 29: 20-25.

[25] Sjöstedt, C.J., and Chen, D.J. Virtual Component Testing for PEM Fuel Cell Systems: An Efficient, High-Quality and Safe Approach for Suppliers and OEM´s. *3rd European PEFC Forum*, Session B09, 2009.

[26] Dzida, M., Dzida, S., Girtler, J. On the possible increasing of efficiency of ship power plant with the system combined of marine Diesel engine, gas turbine and steam turbine, at the main engine – steam turbine mode of cooperation. *Polish Maritime Research* No. 1(59), 2009; Vol. 16, pp.47–52.

Yousri M. A. Welaya, M. Mosleh,
Nader R. Ammar.

Thermodynamic analysis of a combined solid oxide fuel cell
with a steam turbine power plant for marine applications

Nomenclature

CH_4	Methane	$P_{stnet,elec.}$	Net electric output power of steam cycle, kW
CO_2	Carbon dioxide	P_{heat}	Heating loss power, kW
CO	Carbon monoxide	$P_{aircomp.}$	Air compressor required power, kW
C_{pair}	Air specific heat at constant pressure, kJ/kg*k	$P_{fuelcomp.}$	Fuel compressor required power, kW
$C_{pgas.}$	Gas specific heat at constant pressure, kJ/kg*k	PM	Particulate Matter
CV	Fuel calorific value, kJ/kg	PSOFC	Planar SOFC
E_o	Open circuit voltage, volt	PSOFC-IR	Planar SOFC-NG Internal reforming
ECA	Emission control area	$Q_{SH+Evap.}^{gas}$	Heat absorbed by the superheated and saturated exhaust gases streams
EGB	Exhaust gas boiler	$Q_{SH+Evap.}^{steam}$	Heat absorbed by the superheated and saturated steam streams, kW
F	Faraday's constant, Coulomb/mole	Q_{Total}^{gas}	Total heat lost by the exhaust gas stream, kW
h	Enthalpy, kJ/kg.	Q_{Total}^{steam}	Exhaust gas boiler heat duty, kW
$h_{feedwater}$	Feed water to EGB enthalpy, kJ/kg	SOFC	Solid oxide fuel cell
$h_{superheated}$	Superheated steam enthalpy, kJ/kg	SOFC-ST	Solid oxide fuel cell combined cycle
H_2	Hydrogen	SOFCPP	Solid oxide fuel cell power plant
H_2O	Water vapor	SO_x	Sulfur oxides emissions
HFO	Heavy fuel oil	ST	Steam turbine
$h_{fuel,in}$	Inlet fuel enthalpy, kJ/kg	T	Temperature, K.
i_{den}	Current density, mA/cm^2.	TSOFC	Tubular SOFC
IMO	International Maritime Organization	TSOFC-IR	Tubular SOFC-NG Internal reforming
LNG	Liquefied natural gas	U_f	Fuel utilization coefficient
MARPOL	International marine pollution prevention convention	V_{cell}	Fuel cell voltage, volts
$\dot{m}$	Mass flow rate, kg/s	$W_{FC,DC}$	DC power output of the cell stack, kW
m_{Air}	Required Air mass flow rate, kg/s	z	Number of electrons transferred for each molecule of fuel
$m_{hyd.}$	Required hydrogen mass flow rate, kg/s	Greek letters	
$m_{hyd.cons.}$	Hydrogen mass flow rate reacted in fuel cell, kg / s	Δg_f	Change in Gibbs free energy of an electrochemical reaction, kJ /mole
m_{steam}	Steam mass flow rate, kg/s	γ_{air}	Air specific heats ratio
$\dot{m}_{fuel}$	Total input fuel flow rate, kg/s	γ_{gas}	Gas specific heats ratio
NG	Natural gas	η	Efficiency
NO_x	Nitrogen oxides emissions	$\eta_{comb.}$	Combustor efficiency
O_2	Oxygen gas	$\eta_{combined}$	Combined efficiency
p	Pressure, bar	η_{FC}	Fuel cell efficiency
$P_{FC,Ac}$	AC power output of the cell stack, kW	$\eta_{gen.}$	Generator efficiency
P_{st}	Steam cycle output power, kW	η_{st}	Steam turbine cycle efficiency
P_{stnet}	Net output power of steam cycle, kW	$\eta_{isen.}$	Isentropic efficiency
		λ_{Air}	Stoichiometric ratio of air

Yousri M. A. Welaya,
M. Mosleh,
Nader R. Ammar.
Department of Naval Architecture &
Marine Engineering, Alexandria
University, Egypt